Dynamic Article Links

**PAPER**

# Modeling the properties of lanthanoid single-ion magnets using an effective point-charge approach†

José J. Baldoví, Juan J. Borrás-Almenar, Juan M. Clemente-Juan, Eugenio Coronado* and Alejandro Gaita-Ariño*

Herein, we present two geometrical models based on an effective point-charge approach to provide a full description of the lowest sublevels in lanthanoid single ion magnets (SIMs). The first one, named as the Radial Effective Charge (REC) model, evaluates the crystal field effect of spherical ligands, *e.g.* $F^-$, $Cl^-$ or $Br^-$, by placing the effective charge along the Ln–ligand axes. In this case the REC parameters are obtained fitting high-resolution spectroscopic data for lanthanoid halides. The second model, named as the Lone Pair Effective Charge (LPEC) model, has been developed in order to provide a realistic description of systems in which the lone pairs are not pointing directly towards the magnetic ion. A relevant example of this kind is provided by the bis(phthalocyaninato)lanthanoids $[Ln(Pc)_2]^-$. We show that a fit of the magnetic properties of the $[Ln(Pc)_2]^-$ (Ln = Tb, Dy, Ho, Er, Tm and Yb) allows us to extract the LPEC parameters for the lanthanoid complexes coordinated to $sp^2$-nitrogens. Finally, we show that these effective corrections may be extrapolated to a large variety of lanthanoid and actinoid compounds, having either extended or molecular structures.

## Introduction

Over the past few years, the discovery that mononuclear metal complexes can exhibit a single-molecule magnetic (SMM) behavior and new physical phenomena coming from their quantum nature has revitalized the field of Molecular Magnetism.[1] This last generation of SMMs is commonly known as single ion magnets (SIMs). They are usually formed by an anisotropic lanthanoid ion placed in the crystal field created by the surrounding ligands. The first example of such nanomagnets was reported by Ishikawa *et al.* in 2003 in a family of complexes of general formula $[Ln(Pc)_2]^-$ with a 'double-decker' structure and phthalocyaninato anions as ligands (Fig. 1).[2] That seminal work inspired a plethora of more complicated derivatives, *e.g.* triple-deckers,[3] oxidized double-deckers for enhanced magnetic anisotropy[4] or substituted double-deckers for processability, among others.[5] Nowadays, the concept of SIMs has been extended to a growing number of families of mononuclear d-transition metal,[6] lanthanoid[7] and actinoid[8] complexes, but a general theoretical description concerning energy levels, wave functions and magnetic properties is still needed. In contrast with the classical polynuclear SMMs, whose properties are governed by exchange interactions, in SIMs there is a direct relationship between the electronic spectrum resulting from the crystal field splitting and

magnetic properties. For this reason, there is a need for developing simple models, which are able to correlate the structural and electronic features of the metal complex with its SMM properties. Moreover, a reliable description of spin eigenvectors will permit researchers to deal with the potential application of these systems as spin qubits in quantum computing.[1,7d,9] In fact, in this last aspect SIMs are clearly most suitable than the cluster-type SMMs as they exhibit a rich quantum behavior. In this context, the implementation of quantum logic gates in nanomagnets is a motivating challenge that has recently experienced a fast development with both experimental and theoretical results.[10,11,13]

When dealing with SIMs, it is important to note that the magnetic anisotropy required for observing slow relaxation of the magnetization arises from the zero-field splitting of the lanthanoid ion *J* ground state caused by the crystal field. As a consequence, a fairly complex Crystal Field Hamiltonian ($H_{CF}$) must

*Instituto de Ciencia Molecular (ICMol), Universidad de Valencia, C/Catedrático José Beltrán, 2, E-46980 Paterna, Spain.*
*E-mail: coronado@uv.es, gaita@uv.es*
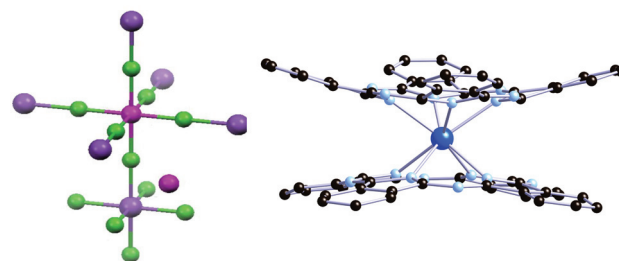†Electronic supplementary information (ESI) available. See DOI: 10.1039/c2dt31411h

**Fig. 1** Left: $Cs_2NaYCl_6$:Er, showing the relative positions of Er (magenta, octahedral), Cl (green), Na (violet), Cs (pink). Right: $[Ln(Pc)_2]^-$.

be properly defined for a full theoretical analysis. According to the literature, it has been proven that even after an intense experimental and theoretical effort, it has rarely been possible to extract more than the nature, strength and orientation of the magnetic anisotropy.[12] Static magnetic properties have been usually reproduced using crude approximations that do not consider most of the terms.[13] In the computational field, Complete Active Space – Self Consistent Field (CASSCF) calculations produce good estimations of the energy levels, but are expensive and only rarely offer general explanations.[14] An inexpensive yet realistic description of the lowest energy sublevels and their wave functions would help to describe their magnetic properties and to rationalize which conditions are favorable for the discovery of new derivatives with such interesting properties.

### Effective point-charge model

In previous work, calculations based on an effective crystal field Hamiltonian that assumes a point-charge electrostatic (PCE) model have permitted us to estimate the whole set of diagonal and extradiagonal crystal field parameters. Such a model parameterizes the crystal field effect generated by the $n$ atoms coordinated to the Ln by using $n$ point charges placed at the corresponding atomic positions. In particular, we have demonstrated the adequacy of this simple model to rationalize the magnetic behavior of several lanthanoid SIMs, mainly those based on polyoxometalates, and even to give some general rules to obtain systems behaving as SMMs or as spin qubits, according to their geometry.[15] Still, a pure PCE model based on a mere geometrical reasoning is expected to be quantitatively correct only for ionic metal complexes. When the nature of the ligand and the orientation of its electronic lone-pairs are taken into account, this simple picture is not realistic and the model needs to be improved. In this work we present an effective point-charge model that intends to overcome this limitation.

Taking a PCE model as a starting point, further studies have been performed to improve the description of the $J$-ground state splitting caused by the crystal field. Some investigations employed effective charges to rationalize intensity parameters of 4f–4f transitions.[16] In that example, effective charges were placed in the middle of the chemical bonds (central ion-ligands), as this location was found to be the best to simulate the ligand field effects and to account for the covalence effects, overcoming the difficulties presented by the simple electrostatic approximation in overestimating the low rank ligand field parameters and underestimating the high rank ones. Other examples with ligand field models[17–20] were based on a certain number of adjustable parameters calculated by *ab initio* methods. These are of worth, not only for elucidative purposes and comparison with experiment, but also because they allow us to predict the ligand field components which cannot be directly obtained from experiment, that is, the odd components of the LF Hamiltonian. Among these models, the simple overlap (SO) model postulates that the ligand field is produced by effective charges, located in the middle of the Ln–ligand bond, which are proportional to the total overlap between Ln and ligand wave functions and to charge factors.[21,22] That model has been applied to a variety of lanthanoid compounds and, in most cases, the charge factors

have been treated as adjustable parameters whose upper limit value is given by the valence of the ligating atom.[23,24]

Despite all these effective corrections, when we deal with nitrogen-coordinated ligands, both the simplest PCE and radial effective improvements seem to be inefficient to describe the magnetic properties of such complexes. A better description of the ligand field would be to consider a dense cloud of tiny charges. This, in principle, could be achieved by means of Density Functional Theory (DFT) calculations. However, for the sake of simplicity we keep the restriction of a single point charge that is allowed to move away from the nitrogen nucleus. Indeed, the effective center of charge of a lone pair is expected to be pretty far from the nucleus. In fact, a key assumption of the electron-pair repulsion model for molecular geometry[25] is that 'a non-bonding or lone-pair is larger and takes up more room on the surface of an atom than a bonding pair'.

In this paper, we present a simple approach to estimate effective charges of F, Cl, Br and N atoms coordinated to lanthanoids by following a corrected PCE model. We distinguish between a Radial Effective Charge (REC) model, for halides, due to their spherical character and a Lone Pair Covalent Effective Charge (LPEC) model in the case of nitrogen. This model is used to provide a full description of the energy level splitting and wave functions of two examples: a high-symmetry solid-state Ho salt, $Cs_2NaHoCl_6$, and the $[Tb(Pc_2)]^-$ SIM (Fig. 1).

## Method

As pointed out above, depending on the ligand character, two different approaches have been performed in order to fit the experimental values namely an REC correction and an LPEC one. In both cases, the starting point of our calculations considers the atomic coordinates of the target compound. Such coordinates are introduced as an input of a software code written in portable *fortran77*.[26] Then, we consider the standard Crystal Field Hamiltonian to parameterize the electric field effect produced by the surrounding ligands, acting over the central ion, which shows the general form:[15]

$$H_{CF}(J) = \sum_{k=2,4,6} \sum_{q=-k}^{k} B_k^q O_k^q = \sum_{k=2,4,6} \sum_{q=-k}^{k} a_k A_k^q \langle r^k \rangle O_k^q \quad (1)$$

where $k$ is the operator order (also called rank or degree) and $q$ is the operator range that varies between $k$ and $-k$, $\langle r^k \rangle$ is the expectation value of $r^k$, and $a_k$ are the $\alpha$, $\beta$ and $\gamma$ Stevens equivalent coefficients for $k = 2, 4, 6$, respectively.[27] $\alpha$, $\beta$ and $\gamma$ are tabulated for the ground state of each lanthanoid ion. Hence, the CF parameters, $A_k^q$ and $B_k^q$, are referred to the ground state as well.

The $A_k^q$ CF parameters can be calculated by the following expression:

$$A_k^q = \frac{4\pi}{2k+1} c_{kq}(-1)^q \sum_{i=1}^{N} \frac{Z_i e^2 Y_{k-q}(\theta_i, \varphi_i)}{R_i^{k+1}} \quad (2)$$

$R_i$, $\theta_i$ and $\varphi_i$ are the effective polar coordinates of the point charge and $Z_i$ is the effective point charge, associated with the $i$-th ligand with the lanthanoid at the origin; $e$ is the electron charge and $c_{kq}$ is a tabulated numerical factor that relates

spherical harmonics $Y_{k-q}$ and Stevens equivalent operators. It is at this point where differences between both approaches do appear.

## Radial effective charge (REC) model

In this approach the ligand is modeled through an effective point charge situated in the axis lanthanoid-coordinated atom at a distance $R$, which is smaller than the real metal–ligand distance. To account for the effect of covalent electron sharing, a radial displacement vector ($D_r$) is defined, in which the polar coordinate $R$ is varied. At the same time, the charge value ($q$) is scanned in order to achieve the minimum deviation between calculated and experimental data, whereas $\theta$ and $\varphi$ remain constant (see Fig. 2 (left)). This model has proven to be very useful to determine the full set of crystal field parameters, energy levels and wave functions when a lanthanoid is surrounded by spherical charges.

## Lone pair effective charge (LPEC) model

The previous approach has been demonstrated to be inappropriate to describe systems where nitrogen is directly bonded to the magnetic center. As we may observe in Fig. 2 (right), the electron lone pair of nitrogen is not located along the radial Ln–N direction, making necessary to define a new displacement vector ($D_h$) named horizontal displacement. Both vectors, $D_h$ and $D_r$, are applied to the original position of each nitrogen nucleus, determining the position of the effective center of charge. Vector $D_r$ is a segment of the distance between the position of the lone pair and the lanthanoid nucleus, and it is defined by the polar coordinate $R$. Note that this latter displacement reflects, like in the REC model, the effective charge resulting from the sharing of the ligand electron density by the lanthanide ion. This correction does possess physical sense due to the fact that the nearest part of the electron cloud to the lanthanoid induces a more marked effect than the areas placed further away. Vector $D_h$ is in the plane NNC containing the ligand atom N and its two covalently bonded atoms (N and C), i.e. the paper plane in Fig. 2. This vector is also parallel to the bisection of the NNC angle, and reflects the effective position of the center of charge of a lone pair. For nitrogen lone pairs, the center of charge is expected to be at a distance between 0.5 and 1.0 Å apart from the nucleus, but the effective "size" of this electron cloud can easily be more than three times larger.[28]
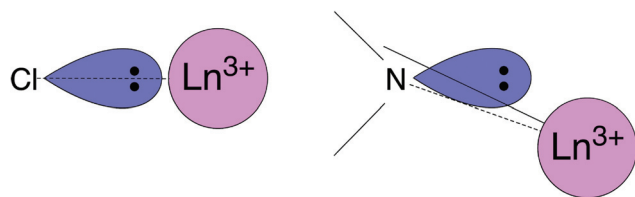


**Fig. 2** Types of orientations between the electronic pair of a ligand and a lanthanoid cation. Left: the lone pair is directly oriented towards the lanthanoid cation. Right: the lone pair is not directly oriented towards the lanthanoid cation. The node in $B_2^0$ is shown as a solid line.

Finally, the minimization procedure searches for the best combination of the displacement and charge corrections to give a local minimum for the root-mean-square (RMS) error from the experiment (energy levels in (1) and (2) and temperature dependence of the $\chi_M T$ product in (3)). In our calculations, we have used a two step optimization. In the first step, we have systematically varied the horizontal displacement between 0.0 and 1.0 Å, the radial one between 0.0 and 1.0 Å, and the charge between 0.0 and 1.5e, obtaining the absolute minimum region in this space. In the second step, we repeated the procedure for a more detailed exploration of the obtained point.

## Results and discussion

### $Cs_2NaYCl_6:Er^{3+}$

Elpasolite structure was chosen because of its simplicity, as the environment of the lanthanoid is perfectly octahedral (see Fig. 1). The splitting of the $Er^{3+}$ $J$ ground state is determined by using the described REC model. For the determination of the effective charge of the chloride atoms, experimental data taken from the optical absorption and emission results reported by Foster and Richardson[29] for a doped $Cs_2NaYCl_6:Er^{3+}$ system have been employed.

In this highly symmetric environment, the non-vanishing CF terms are $B_4^0$, $B_6^0$, $B_4^4$ and $B_6^4$. Since there the $B_4^0/B_6^0$ (or $B_4^4/B_6^4$) ratio is fixed, the number of independent parameters is fixed to 2. Thus, a fitting of the high-resolution spectroscopic data of the Er derivative to the REC model results in an absolute error minimum at $Z_i = -0.41$ and $d_r = 0.88$ Å.

This correction obtained for the Er case has been applied without any modification to calculate the energy levels of the whole series, from Tb to Yb. The agreement between the REC model and the experiment is excellent. Moreover, the Er-based correction can also provide excellent results for the uranium analogue. The worst agreement with the Er-based correction has been found for the Dy derivative, so we chose this case for illustration. Fig. 3 compares the experimental energy levels of $Cs_2NaYCl_6:Dy^{3+}$ with the basic PCE prediction and with the REC model. As we can see, the PCE model totally fails to quantitatively describe the energy spectrum for Dy. In contrast, the REC model closely reproduces the experimental energy spectrum. Thus, the energies of the first excited levels are accurately calculated by the model, while those corresponding to the higher energy levels differ from the experimental energies by less than a 15%.

We find that the parameters are not completely independent. For the whole series, the minimal errors (in the ranges $0 < Z_i < 1.5$, $0 < D_r < 1.5$) are found near the relation:

$$D_r = \sqrt{\frac{1}{Z_i + 0.25} - 0.4} \qquad (3)$$

Calculations over the same structure with $Br^-$ and $F^-$ have also been carried out following the same model with $Cs_2NaYF_6$:$Yb^{3+}$ and $Cs_2NaYBr_6$:$Yb^{3+}$. For $F^-$, one obtains $Z_i = -0.20$ and $D_r = 1.03$ Å as correcting parameters. For $Br^-$, the parameters are $Z_i = -0.45$ and $D_r = 0.90$ Å. With these new data, and
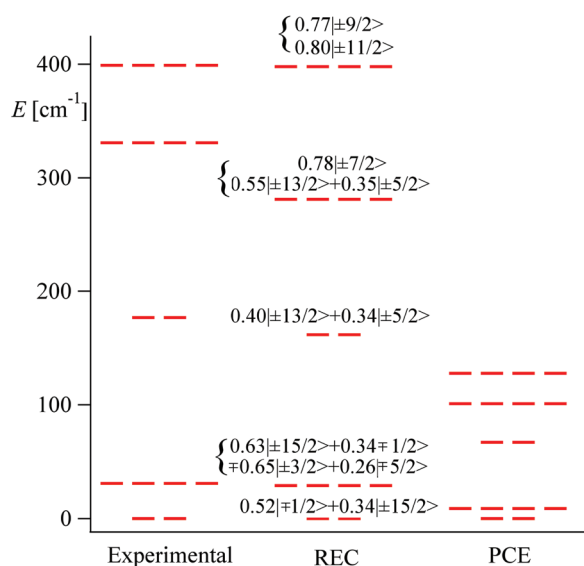
**Fig. 3** Observed energy sublevel data of $Cs_2NaYCl_6:Dy^{3+}$ compared with REC (Er-based correction) and PCE models.

assuming a monotonous variation for the F–Cl–Br series, we estimate for $Cl^-$ the parameters $Z_i = 0.26$ and $D_r = 1.00$ Å.

## $[Tb(Pc_2)]^-$

For the study of the LF effect of the phthalocyaninato ligand, the LPEC correction is required. Here we need to emphasize the difference between our present fitting procedure and the one originally used by Ishikawa et al.[30] Previous work used the ligand field terms as fitting parameters, and to avoid overparametrization, a linear dependence of all three diagonal parameters with the number of electrons was simply assumed. Instead, our fitting parameters are only the position and value of the point charges. That enables us to introduce a richer Hamiltonian without such overparametrization problems and without assuming arbitrary variations of the ligand field terms. Still, for simplicity, and because of the lack of crystal structures for the whole series, we slightly idealize the structure by assuming a $C_4$ symmetry but keeping the experimental torsion angle between the two phthalocyaninato ligands. This idealization will only affect small extradiagonal terms that will alter the mixing but have almost no effect on the $\chi_M T$ values. In this simplified environment, the non-vanishing CF terms are $B_2^0$, $B_4^0$, $B_6^0$, $B_4^4$ and $B_6^4$. With this assumption and after applying displacement vectors and charge scanning, one generally obtains an excellent agreement with the experimental $\chi_M T$ curves of the whole series (see Fig. 4). The limitations of this three-parameter simultaneous fit of six experimental curves are reflected in the poor agreement of the low-temperature behavior of the dysprosium compound; alternate fits (not shown) are better for dysprosium but worse overall. The procedure results in the following set of parameters: $Z_i = -0.63$, horizontal displacement $D_h = 0.195$ Å and radial displacement $D_r = 0.48$ Å. Compared with the nuclear positions of the nitrogen atoms, this horizontal displacement means that the effective barrier has crossed the node at the "magic" polar angle $\theta = 54.73°$. This translates into a sign change of the ZFS
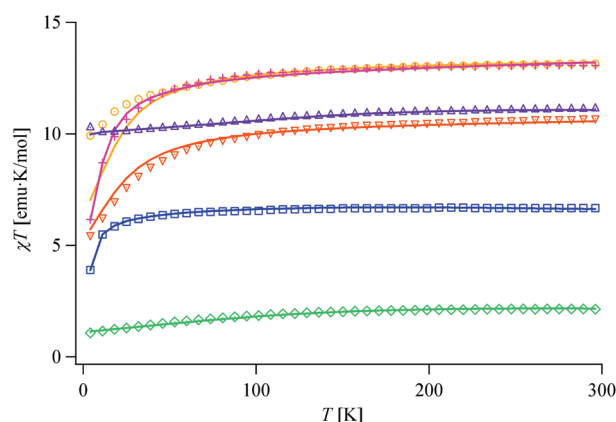


**Fig. 4** Simultaneous fitting of the experimental magnetic properties of the series of $[Ln(Pc)_2]$ SIMs from the LPEC model: Dy (○), Ho (+), Tb (△), Er (▽), Tm (□) and Yb (◇).

parameter $D$ (where $D = 3B_2^0$) so that it is negative for $Tb^{3+}$ accounting for the SMM behavior observed in this compound. The total displacement of approximately 0.6 Å is well within the expected volume of the electron cloud, not very far from its charge centroid. In fact, for nitrogen lone pairs, the center of charge is expected to be at a distance between 0.5 and 1.0 Å apart from the nucleus, but the effective "size" of this electron cloud can easily be, depending on its definition, more than three times larger.[31] The effective charge $Z$ is also reasonable, and in full agreement with previous DFT calculations, which resulted in a natural bond orbital charge $q_{NBO} = -0.7$ for $[Y(Pc)_2]^-$.[32] Note that while this correction is generally a clear improvement for $(sp^2)N$ ligands over the simple PEC model, the theoretical treatment of markedly different ligands such as the azide radical $N_2^{3-}$ would benefit from a dedicated correction following the same procedure.

Applying the whole-series fit to the Terbium derivative, we obtain a well-isolated ground state doublet composed of $|+6\rangle$ and $|-6\rangle$, with the rest of the sublevels excited by more than 300 $cm^{-1}$ and bunched up in a window of less than 150 $cm^{-1}$. This picture is coherent with its known SIM properties, allowing the slow relaxation of the magnetization. Ishikawa provided essentially the same description. In that study, the first excited sublevel lies at about 400 $cm^{-1}$ and the lowest substrates are $|+6\rangle$ and $|-6\rangle$. A crucial difference between both energy level schemes is the effect of the fourth-range extradiagonal parameters ($B_4^4$ and $B_6^4$). These parameters enable a mixing between the $|+6\rangle$ and $|-6\rangle$ doublet at zero field. Indeed, with a pseudoaxial LF Hamiltonian all doublets have pure $M_J$ values, while our approach quantifies the Hamiltonian extradiagonal terms and thus the $M_J$ mixing. In this case, this mixing arises from three consecutive steps when applying the fourth-range parameters, whose operators contain the fourth power of the staircase operator e.g. $O_4^4 = 1/2(J_+^4 + J_-^4)$. Thus, the applications of these parameters mix $|+6\rangle$ with $|+2\rangle$, then with $|-2\rangle$ and finally, with $|-6\rangle$, and analogously, $|-6\rangle$ is mixed with $|+6\rangle$, passing through the same $M_J$ states. That is the reason why the mixing is very weak and cannot give rise to a noticeable tunnel splitting, as does occur in other examples of the literature.[33] In a different manner, it also means that a minimal longitudinal

**Table 1**  Energies and modulus of the contribution of each $M_J$ to the wave-functions of the ground state multiplets of TbPc$_2$

| Energy (cm$^{-1}$) | Wave function | | |
|---|---|---|---|
| 0 | **0.79·\|−6>** | **0.61·\|6>** | |
| 0 | **0.61·\|−6>** | **0.79·\|6>** | |
| 321 | 0.01·\|−4> | **1.00·\|0>** | 0.01·\|4> |
| 339 | 0.03·\|−5> | **1.00·\|−1>** | 0.03·\|3> |
| 339 | 0.03·\|−3> | **1.00·\|1>** | 0.03·\|5> |
| 342 | **1.00·\|−5>** | 0.03·\|−1> | |
| 342 | 0.03·\|1> | **1.00·\|5>** | |
| 383 | **0.71·\|−2>** | **0.71·\|2>** | |
| 391 | **0.71·\|−2>** | **0.71·\|2>** | |
| 440 | **1.00·\|−3>** | 0.03·\|1> | |
| 440 | 0.03·\|−1> | **1.00·\|3>** | |
| 450 | **0.71·\|−4>** | **0.71·\|4>** | |
| 450 | **0.71·\|−4>** | **0.71·\|4>** | |

**Table 2**  Energies and modulus of the contribution of each $M_J$ to the wave-functions of the ground state multiplets of DyPc$_2$

| Energy (cm$^{-1}$) | Wave function | | |
|---|---|---|---|
| 0 | **1.00·\|−11/2>** | 0.01·\|−3/2> | |
| 0 | 0.01·\|3/2> | **1.00·\|11/2>** | |
| 42 | **1.00·\|−13/2>** | 0.03·\|−5/2> | |
| 42 | 0.03·\|5/2> | **1.00·\|13/2>** | |
| 70 | **1.00·\|−9/2>** | 0.01·\|−1/2> | |
| 70 | 0.01·\|1/2> | **1.00·\|9/2>** | |
| 167 | 0.03·\|−13/2> | **1.00·\|−7/2>** | |
| 167 | **1.00·\|7/2>** | 0.03·\|15/2> | |
| 252 | 0.03·\|−15/2> | **0.99·\|−5/2>** | 0.15·\|3/2> |
| 252 | 0.15·\|−3/2> | **0.99·\|5/2>** | 0.03·\|15/2> |
| 313 | 0.01·\|−11/2> | **0.99·\|−3/2>** | 0.15·\|5/2> |
| 313 | 0.15·\|−5/2> | **0.99·\|3/2>** | 0.01·\|11/2> |
| 341 | 0.01·\|−9/2> | **1.00·\|−1/2>** | 0.03·\|7/2>  0.03·\|15/2> |
| 341 | 0.03·\|−15/2> | 0.03·\|−7/2>  **1.00·\|1/2>** | 0.01·\|9/2> |
| 347 | **1.00·\|−15/2>** | 0.03·\|−7/2> | 0.03·\|1/2> |
| 347 | 0.03·\|−1/2> | 0.03·\|7/2> | **1.00·\|15/2>** |

**Table 3**  Summary of the effective charge corrections found for the different ligands

| | $Z_i$ | $D_h$ (Å) | $D_r$ (Å) |
|---|---|---|---|
| F$^-$ | −0.20 | n.a. | 1.03 |
| Cl$^-$ | −0.26 | n.a. | 1.00 |
| Br$^-$ | −0.45 | n.a. | 0.90 |
| (sp$^2$)N | −0.63 | 0.195 | 0.48 |

useful theoretical general tool for the rational design of SIMs and spin qubits based on mononuclear lanthanoid complexes.[18] Here we went a step further and presented two alternative improvements to this model in order to take into account not only the geometrical arrangement of the coordinated ligands, but also their orbital details. We have shown that a Radial Effective Charge (REC) model is sufficient for spherical ligands such as halides. In fact, this model has provided an excellent description of the low-lying energy level splitting and associated wavefunctions in lanthanoid compounds based on these ligands. In turn, we have shown that a Lone Pair Effective Charge (LPEC) model is needed for ligands, which coordinate through a non-radial lone pair, such as the sp$^2$ nitrogen atoms of the phthalocyaninato anion.

Compared with the approach initially used by Ishikawa to extract the crystal field parameters from a fit of the magnetic properties of the series [Tb(Pc$_2$)]$^-$, our approach presents important advantages. The main one is that here the fitting parameters are not the crystal field parameters. Instead, they refer to molecular parameters such as the effective charge on the ligand and its distance to the lanthanoid, which have a clear chemical meaning. This has two relevant consequences. First, it facilitates distinguishing meaningful solutions from mathematical artifacts by chemical common sense. Second, it allows the application of these tabulated parameters, which are characteristic of each ligand, to any other non-ideal structures to produce the complete set of off-diagonal ligand field terms without any free parameter. Indeed, we obtain corrections (Table 3) for F$^-$, Cl$^-$, Br$^-$ and (sp$^2$)N which can be used to enhance in a simple and affordable way the quality of a point-charge model. This makes our results useful for a wide variety of lanthanoid compounds, being easily extrapolated to the case of actinides (mononuclear uranium complexes, for example).

magnetic field – necessary to find a level crossing where tunneling is not forbidden by the nuclear spins – will recover the purity of the $M_J$ states. Due to these peculiarities, [Tb(Pc$_2$)]$^-$ is an interesting example where the SIM behavior is not destroyed by extradiagonal terms allowing a mixing within the ground state.

Tables 1 and 2 show the energy level scheme for the Tb and Dy derivatives, as well as the main terms of the wave functions. For space reasons, we skip a detailed comparison between our energy level scheme and the associated wave functions (Tables S1 through S4 in ESI†) for the rest of the metals and the results reported in ref. 33. Here we just highlight the key similarities and differences for each lanthanoid. A first general difference is that our calculations consistently result in smaller energy level splitting, ranging from 450 cm$^{-1}$ for Tb to 275 cm$^{-1}$ for Ho and Er, compared with Ishikawa's nearly 600 cm$^{-1}$ for Tb and about 400 cm$^{-1}$ for Ho and Er. As already pointed above, a second general difference is the presence of the fourth-range extradiagonal parameters, which have more or less pronounced consequences depending on the nature of the ground state.

## Conclusions

In a previous work, we developed an inexpensive point-charge evaluation of the ligand field Hamiltonian, which provided a

## Notes and references

1 J. M. Clemente-Juan, E. Coronado and A. Gaita-Ariño, *Chem. Soc. Rev.*, 2012, DOI: 10.1039/c2cs35205b.
2 N. Ishikawa, M. Sugita, T. Ishikawa, S. Y. Koshihara and Y. Kaizu, *J. Am. Chem. Soc.*, 2003, **125**, 8694.

3 N. Ishikawa, S. Otsuka and Y. Kaizu, *Angew. Chem., Int. Ed.*, 2005, **44**, 731.

4 N. Ishikawa, Y. Mizuno, S. Takamatsu, T. Ishikawa and S. Y. Koshihara, *Inorg. Chem.*, 2008, **47**, 10217.

5 J. Gómez-Segura, I. Díez-Pérez, N. Ishikawa, M. Nakano, J. Veciana and D. Ruiz-Molina, *Chem. Commun.*, 2006, 2866.

6 (*a*) W. H. Harman, T. D. Harris, D. E. Freedman, H. Fong, A. Chang, J. D. Rinehart, A. Ozarowski, M. T. Sougrati, F. Grandjean, G. J. Long, J. R. Long and C. J. Chang, *J. Am. Chem. Soc.*, 2010, **132**, 18115–18126; (*b*) J. M. Zadrozny and J. R. Long, *J. Am. Chem. Soc.*, 2011, **133**, 20732–20734.

7 (*a*) M. A. AlDamen, J. M. Clemente-Juan, E. Coronado, C. Martí-Gastaldo and A. Gaita-Ariño, *J. Am. Chem. Soc.*, 2008, **27**, 3650; (*b*) M. A. Aldamen, S. Cardona-Serra, J. M. Clemente-Juan, E. Coronado, A. Gaita-Ariño, C. Martí-Gastaldo, F. Luis and O. Montero, *Inorg. Chem.*, 2009, **48**, 3467; (*c*) F. Luis, M. J. Martínez-Pérez, O. Montero, E. Coronado, S. Cardona-Serra, C. Martí-Gastaldo, J. M. Clemente-Juan, J. Sesé, D. Drung and T. Schurig, *Phys. Rev. B*, 2010, **82**, 060403; (*d*) M. J. Martínez-Pérez, S. Cardona-Serra, C. Schlegel, F. Moro, P. J. Alonso, H. Prima-García, J. M. Clemente-Juan, M. Evangelisti, A. Gaita-Ariño, J. Sesé, J. van Slageren, E. Coronado and F. Luis, *Phys. Rev. Lett.*, 2012, **108**, 247213; (*e*) S. Jiang, B. Wang, H. Sun, Z. Wang and S. Gao, *J. Am. Chem. Soc.*, 2011, **133**, 4730–4733; (*f*) S. Jiang, B. Wang, G. Su, Z. Wang and S. Gao, *Angew. Chem., Int. Ed.*, 2010, **49**, 7448–7451; (*g*) P. E. Car, M. Perfetti, M. Mannini, A. Favre, A. Caneschi and R. Sessoli, *Chem. Commun.*, 2011, **47**, 3751.

8 (*a*) J. D. Rinehart and J. R. Long, *J. Am. Chem. Soc.*, 2009, **131**, 12558; (*b*) J. D. Rinehart, K. R. Meihaus and J. R. Long, *J. Am. Chem. Soc.*, 2010, **132**, 7572–7573; (*c*) M. A. Antunes, L. C. J. Pereira, I. C. Santos, M. Mazzanti, J. Marçalo and M. Almeida, *Inorg. Chem.*, 2011, **50**, 9915–9917.

9 (*a*) A. Ardavan and S. J. Blundell, *J. Mater. Chem.*, 2009, **19**, 1754; (*b*) F. Troiani and M. Affronte, *Chem. Soc. Rev.*, 2011, **40**, 3119; (*c*) P. C. E. Stamp and A. Gaita-Ariño, *J. Mater. Chem.*, 2009, **19**, 1718.

10 S. Bertaina, *et al.*, *Nat. Nanotechnol.*, 2007, **2**, 39.

11 F. Troiani and M. Affronte, *Chem. Soc. Rev.*, 2011, **40**, 3119–3312.

12 K. Bernot, J. Luzon, L. Bogani, M. Etienne, C. Sangregorio, M. Shanmugam, A. Caneschi, R. Sessoli and D. Gatteschi, *J. Am. Chem. Soc.*, 2009, **131**, 5573.

13 N. Magnani, R. Caciuffo, E. Colineau, F. Wastin, A. Baraldi, E. Buffagni, R. Capelletti, S. Carretta, M. Mazzera, D. T. Adroja, M. Watanabe and A. Nakamura, *Phys. Rev. B*, 2009, **79**, 104407.

14 J.-L. Liu, K. Yuan, J.-D. Leng, L. Ungur, W. Wernsdorfer, F. S. Guo, L. F. Chibotaru and M.-L. Tong, *Inorg. Chem.*, 2012, **51**, 8538.

15 J. J. Baldoví, S. Cardona-Serra, J. M. Clemente-Juan, E. Coronado, A. Gaita-Ariño and A. Palii, submitted.

16 O. L. Malta, M. A. Couto dos Santos, L. C. Thompson and N. K. Ito, *J. Lumin.*, 1996, **69**, 77.

17 D. Garcia and M. Faucher, in *Hand Book on the Physics and Chemistry of Rare Earths*, ed. K. A. Gshneidner Jr. and L. Eyring, 1995, ch. 144, vol. 21.

18 C. K. Jørgensen, R. Pappalardo and H. B. Schmidtke, *J. Chem. Phys.*, 1963, **39**, 1422.

19 D. J. Newman, *Adv. Phys.*, 1971, **20**, 197.

20 C. A. Morrison, Lectures on Crystal Field Theory HDL-SR-82-2 Report, 1982.

21 O. L. Malta, *Chem. Phys. Lett.*, 1982, **87**, 27.

22 O. L. Malta, *Chem. Phys. Lett.*, 1992, **88**, 353.

23 S. Jank, H. Reddmann and H.-D. Amberger, *Spectrochim. Acta, Part A*, 1998, **54**, 1651.

24 P. Porcher, M. C. Dos Santos and O. Malta, *Phys. Chem. Chem. Phys.*, 1999, **1**, 397.

25 R. J. Gillespie, *J. Chem. Educ.*, 1970, **47**, 18.

26 J. J. Baldoví *et al.*, unpublished results.

27 K. W. H. Stevens, *Proc. Phys. Soc.*, 1952, **65**, 209.

28 M. A. Robb, W. J. Haines and I. G. Csizmadia, *J. Am. Chem. Soc.*, 1973, **95**, 42.

29 D. R. Foster and F. S. Richardson, *J. Chem. Phys.*, 1985, **82**, 1085.

30 N. Ishikawa, Y. Mizuno, S. Takamatsu, T. Ishikawa, S. Y. Koshihara and Y. Kaizu, *J. Phys. Chem. B*, 2004, **108**, 11265.

31 M. A. Robb, W. J. Haines and I. G. Csizmadia, *J. Am. Chem. Soc.*, 1973, **95**, 42.

32 Y. Zhang, X. Cai, Y. Zhou, X. Zhang, H. Xu, Z. Liu, X. Li and J. Jiang, *J. Phys. Chem. A*, 2007, **111**, 392.

33 (*a*) S. Cardona-Serra, J. M. Clemente-Juan, E. Coronado, A. Gaita-Ariño, A. Camón, M. Evangelisti, F. Luis, M. J. Martínez-Pérez and J. Sesé, *J. Am. Chem. Soc.*, 2012, DOI: 10.1021/ja305163t; (*b*) S. Ghosh, S. Datta, L. Friend, S. Cardona-Serra, A. Gaita-Ariño, E. Coronado and S. Hill, *Dalton Trans.*, DOI: 10.1039/C2DT31674A.